AT&T Technical Journal
Vol. 64, No. 8, October 1985
Printed in U.S.A.

# Equalizing Without Altering or Detecting Data

By G. J. FOSCHINI*

(Manuscript received August 27, 1984)

For terrestrial digital radio systems that use Quadrature Amplitude Modulation, the idea of adapting equalizers to multipath distortion, without relying on accurate data estimates, is attractive. Prompt adaptation following a severe fade, when accurate data estimates are unavailable, is useful for reducing outage time. To avoid processing and administrative overhead, the adaptation method should not involve violating the transmitted signal with the insertion of equalizer training signals. We approach this kind of equalization by building on an algorithm of D. Godard (IEEE Transactions on Communications, November 1980)[1] that was devised for voiceband polling networks. The method involves a very simple tap update procedure. However, the technique lacks the foundation of the years of analysis and experimentation that underlie least-mean-square adaptation algorithms. The main purpose of this paper is to present new findings, including (1) a proof that the algorithm, thought to require special equalizer initialization, converges regardless of initialization (this offers useful flexibility in digital radio systems, since, after a severe fade, the algorithm could start with any tap misalignment); (2) a preliminary look at convergence speed suggesting the possibility of significant outage reduction; (3) an algorithm that provides phase coherence (the original algorithm requires a follow-on phase-locked loop); and (4) an algorithm for cross-polarization cancellation as well as equalization.

## I. INTRODUCTION

### *1.1 The problem of prompt data detection*

Consider a Quadrature Amplitude Modulation (QAM) digital radio signal (or a dually polarized QAM pair) propagating through a medium

* AT&T Bell Laboratories.

subject to slowly, randomly varying, frequency selective fades (and cross-polarization coupling). On certain occasions the loss of signal can be so complete that a theoretically optimum receiver could not detect the data. Subsequently, a strong signal returns, but carrier and timing may have wandered and the medium may have significantly changed its dispersive character. The objective is to detect the data symbols forthwith as the signal strength returns.

It is the uncertainty about the various features of the received signal, apart from the inherent uncertainty associated with the information symbols (and additive noise), that slows the recapture process. Carrier frequency and phase, and timing frequency and phase are all to some degree uncertain. Moreover, the $2 \times 2$ matrix transfer characteristic of the dispersive medium (the diagonal elements describe the co-polarization transfer characteristics and the off-diagonal terms express the couplings between polarizations) is also uncertain. This medium must be equalized to enable accurate data detection. During the bootstrapping, reliable data estimates are unavailable. Consequently, data-directed Minimum-Mean-Square Error (MMSE) equalization is not feasible.

In this paper a method of equalization is analyzed that does not require the availability of data estimates. The method involves tap adjustments based on simple computations using samples of the received QAM signal and of the equalizer output. For simplicity, in the following sections equalization (along with cross-polarization cancellation) is considered in isolation assuming carrier and timing recovery have somehow been accommodated. We stress that equalization is one part of the bootstrapping process. At the time of this writing, carrier recovery is a topic of research. One promising approach employs a quartic nonlinearity. Later we will say more about carrier recovery. Regarding timing frequency, we anticipate that the squared-envelope method is adequate in most applications. Practical realizations of the systems we analyze are assumed to employ a sufficient number of fractionally spaced taps to be quite robust to timing phase.

### *1.2 Are probing tones not needed?*

The approach to equalization that we treat leaves the standard form of the transmitted signal inviolate. (In contrast, one could monitor the medium with real-time measurements and adjust equalizers on the basis of the measurements.) Is the standard (no modification at the transmitter) signal already a media probing signal? Is it also a control signal that arranges for equalizers and cross-polarization cancellors to automatically align in response to reasonable real-time, digital signal processing? A practical affirmative answer would enable one to avoid

the processing and administrative overhead associated with altering the form of the transmitted signal.

### *1.3 Outline of results*

In this paper we take an approach to equalization, without altering or detecting data, that was originally designed for expediting start-up in equalizers in voice band polling networks. The method, originated by D. Godard,[2] involves a very simple tap update procedure and for that reason is especially attractive. [See Ref. 3 for an earlier paper providing a method for PAM (but not QAM) signals. Related research has been conducted.[4-6]] The algorithm assumes the average squared constellation vector is zero and is presented in Section IV. First some background is needed. In Section II the basic model for single polarization transmission is presented. Section III discusses a general view of the tap evolution that will be used.

Godard's algorithm lacks the foundation of the years of analysis and experimentation that underlie least-mean-square adaptation algorithms. The main purpose of this paper is to present new findings on the mathematical theory of this little-understood algorithm.

The algorithm was thought to require special tap initialization to converge. We show that the algorithm converges regardless of initialization (Section V). This flexibility is significant given the vagaries of tap misalignments that could be associated with severe channel fading.

In Section VI we take a preliminary look at the subject of convergence speed. This is accomplished by reinterpreting published numerical work[1] (aimed at voiceband systems) for digital radio applications. While a mathematical analysis of the transient behavior seems intractable, Section VI explains that considerable insight can be obtained from the analysis of a much simpler related problem.

Two new algorithms related to the Godard algorithm are given. The first (Section VII) provides phase coherence as part of the equalization process for hypothetical systems employing highly stable oscillators. The original algorithm required a follow-on phase-locked loop. Section VIII presents an algorithm that provides for cross-polarization cancellation as well as equalization.

Throughout much of this paper the mathematical theory idealizes assuming an infinite tap equalizer. This is because it is very awkward to deal analytically with the finite tap case. One is left wondering if there is any pitfall associated with the finite tap algorithm. The current status of this issue is addressed in Section IX. There is some evidence that the infinite tap—finite tap contrast is nearly as tame as it is with MMSE equalization.

A second purpose of this paper is to answer the question of whether the potential for using the aforementioned algorithm in digital radio

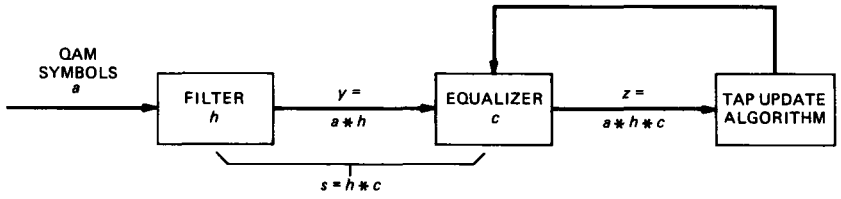


a, h, c, y, z AND s ARE DOUBLY INFINITE COMPLEX SEQUENCES

Fig. 1—Simplified baseband model.

systems is significant enough to warrant detailed study. An affirmative answer is given.

A discussion is given in Section X. The Appendix contains information on QAM constellation moments.

## II. THE MODEL

Since our primary goal is the presentation of theoretical results, a simple setting is used. We work with the equivalent baseband model shown in Fig. 1. The complex data sequence is denoted $a$. The elements of $a = (\cdots a_0, a_1, \cdots)$ represent independent identically distributed choices from a QAM constellation, each point of which is equally likely. We normalize so that $E|a_n|^2 = 1$.

The complex sequence $h$ represents samples of the impulse response of the transmitter and medium combination. The sequence $c$ represents the complex equalizer taps. Using the $*$ symbol for convolution, the sampled impulse response of the channel and equalizer in combination is denoted $s = h * c$, the received data is denoted $y = a * h$, and the sequence after the equalizer is $z = a * h * c$. This notation is consistent with the notation of Ref. 1.

Also, $h$ is assumed to have a continuous Fourier transform devoid of spectral nulls. Consequently, $h$ has a convolution inverse $h^{-1}$ satisfying $h * h^{-1} = \overline{0}1\overline{0}$. By $\overline{0}$ we mean an infinite sequence of zeroes, left directed if preceding a number and right directed if following a number. If $\overline{0}$ is written without abutting a number, it means the sequence of zeroes extending from $-\infty$ to $+\infty$.

A more refined model of the terrestrial digital radio environment would include additive white Guassian noise at the input to the receiver. However, the major interest in this paper is in prompt reestablishment of adequate equalization *after* a cataclysmic event during which the data-detection capability was completely lost (so $P_e \rightarrow 1/2$). The situation is that the medium, despite the presence of additive noise, has the potential of providing adequate performance if only the

equalizer could be properly aligned. In such situations the s/n is generally so large that optimal MMSE equalizer including noise effects is only slightly better than the inverse equalizer,[7] which neglects noise. Once the equalization can provide for a $P_e$ in the neighborhood of 0.1, conventional linear MMSE equalization is an option. To be prudent, unless stated otherwise, this option is assumed. So neglecting the noise is not a substantive shortcoming of the analysis. MMSE Decision Feedback (DF) equalization is an alternative option. The bane of DF has been the possibility of the detection process entering a disasterous error propagation mode. With Godard's algorithm as a fallback, the error propagation is no longer disasterous. The theoretical performance of DF is superior to linear equalization.[8-10] Therefore, in a severe fade, DF helps in forestalling the failure of the decision-directed mode. However, in some important digital radio applications the theoretical advantage of DF over linear is marginal.[7]

## III. VECTOR FIELD FOR EQUALIZER TAP EVOLUTION

Generally a tap update is a random vector. The subject of "convergence" of a tap update procedure prompts several interesting questions. What is the underlying trend in the tap evolution? If the tap setting is tending to some target region, how long does it take to get there? What is the long-term equilibrium distribution of the tap settings? Recasting the last question less mathematically: Do the tap settings significantly stray from the target region once they get there? These are difficult questions. In this paper we will primarily attack the first question, say a little about the second, and defer the third. The target region can be defined as constituting those settings for which MMSE can commence. We proposed above that MMSE be used when possible. Consequently, for the third question we defer to MMSE theory.

To address the first question, we shall deal with the mathematical abstraction of vector fields in tap space. That is, at each point in tap space there is a vector, that, when added to the current vector of tap settings, points to where the taps should nominally be set in the immediate future. Anticipating that time spans of interest in tap bootstrapping processes involve over $10^4$ symbols, it is sometimes useful to approximate and represent tap evolution in continuous rather than discrete time. The vectors are smooth functions of the taps. The relative magnitudes of the vectors relate to the relative speed of change of the taps.

The fields of interest to us are conservative, that is, they are derived by taking the gradient of a potential function $\phi$. The gradient depends on the current tap setting and the channel-impulse response. We stress that in implementations the channel response is not known and the tap changes (gradients) are derived from readily accessible random

variables whose mean values are the desired quantities. (This is the so-called stochastic gradient approach. Conventional MMSE utilizes a stochastic gradient approach requiring accurate data estimates.)

The potential functions we will work with are fourth-degree polynomials in the tap gains and their complex conjugates. Exceptional points, where the field vector is a zero vector, are called stationary points. For potential functions such as fourth-degree polynomials the Hessian matrix

$$\mathscr{H} = \left( \frac{\partial^2 \phi}{\partial \bar{c}_l \partial c_m} \right)$$

types the stationary points. (We are using a bar here for complex conjugation.) This typing stems from a power-series expansion about a stationary point and is as follows:

positive semidefinite $\leftrightarrow$ local minimum
negative semidefinite $\leftrightarrow$ local maximum
indefinite $\leftrightarrow$ unstable equilibrium.

In the sequel, when we say that an algorithm "converges" to some set, we mean that the set constitutes the points of stable equilibrium of the corresponding vector field.

The stochastic gradients of $|z_n|^4$ and $|z_n|^2$ will be used later. We record them for reference for even positive powers $Q$. We obtain (similar to Ref. 1)

$$\frac{\partial |z_n|^Q}{\partial \bar{c}_k} = \frac{\partial}{\partial \bar{c}_k} [(y'c)(\bar{y}'\bar{c})]^{Q/2} = \frac{Q}{2} [(y'c)(\bar{y}'\bar{c})]^{(Q/2)-1} (y'c)\bar{y}_k.$$

The prime denotes transpose and the bar denotes conjugation. Since $(Q/2) - 1$ is a nonnegative integer the computation of the stochastic gradient of $|z_n|^Q$ involves only multiplications of readily accessible quantities. These quantities are the tap settings and the vector of tap outputs. We note that the taps evolve so that the vector $c$ is a function of time and the notation has suppressed that dependence thus far.

## IV. DESCRIPTION OF GODARD'S QUARTIC ALGORITHM

In this section we review the algorithm of Ref. 1 for updating equalizer taps, for which, remarkably, data estimates are not required. The algorithm, if properly initialized, is known to converge to a vector of the form $h * c = (\cdots 0, e^{j\theta}, 0, 0, \cdots)$, which is the ideal Nyquist response, except for the presence of an arbitrary phase $\theta$. In other words, the algorithm converges so that $z$ is the same as $a$ except that the constellation needs to be rotated into position. The four-fold ambiguity associated with positioning the constellation is not a prob-

lem since the data is assumed to be differentially encoded at the transmitter.

Let $c_{[n]}$ denote the tap vector at time $n$. The tap update procedure is based on a gradient minimization of

$$\phi(c_{[n]}) = E(|z_n|^2 - R)^2, \tag{1}$$

where $R = E|a_n|^4/E|a_n|^2 = E|a_n|^4$ is a constant depending only on the signal constellation. Thus the tap update procedure is

$$c_{[n+1]} = c_{[n]} - \lambda \bar{y}_n z_n(|z_n|^2 - R), \tag{2}$$

where $\lambda$ is the step size.

One way to motivate eq. (1) is to consider

$$\hat{\phi} = E(|z_n|^2 - |a_n|^2)^2 \tag{3}$$

as an error criterion. Overlook, for a moment, that estimates of $|a_n|^2$ are not available at the receiver immediately after a severe fade. $\hat{\phi}$ has some nice features. After all it measures zero when $z_n = a_n$. The systems we are dealing with are nominally linear, so that it seems reasonable to speculate that when $\hat{\phi}$ is zero, then the system is ideally equalized modulo a rotation of the constellation. We must replace $|a_n|^2$ in (3) by a more reasonable quantity. We replace it by a constant chosen to make the two expectations in (1) and (3) have substantial agreement when expressed in more fundamental form in terms of $h$ and $c$. (See Ref. 1 for details.) This completes the interpretation of the choice of $R$.

Recalling that $s = h * c$, the potential $\phi(c)$ is expressed as

$$\phi(c) = 2\,(\sum |s_k{}^2)^2 - (2 - E|a_n|^4) \sum |s_k|^4 - 2E|a_n|^4 \sum |s_k|^2 + (E|a_n|^4)^2. \tag{4}$$

Let $L^2$ be the number of constellation points and recall the normalization $E|a_n|^2 = 1$. Regarding $s = h * c$ as the independent variable, we have

$$\phi(s) = 2\,(\sum |s_k|^2)^2 - \left(\frac{3(L^2+1)}{5(L^2-1)}\right) \sum |s_k|^4 - 2\left(\frac{7L^2-13}{5(L^2-1)}\right) \sum |s_k|^2 + \left(\frac{7L^2-13}{5(L^2-1)}\right)^2. \tag{5}$$

The equality (4), comes from straightforward harmonic analysis (it appears in Ref. 1) and equality (5) uses the Appendix.

In the following sections new results are presented on the theory of quartic algorithms.

## V. CONVERGENCE OF THE QUARTIC ALGORITHM

In the previous section we mentioned that the algorithm converges if it is properly initialized. Now we will show that such initialization is not needed for convergence. In a certain sense the algorithm will converge regardless of the initialization. More precisely, we show that the only loci of stability of the vector field in tap space are the family of sets

$$E_k = \{c \mid c * h = e^{j\theta}(\bar{0}1_k\bar{0}), \quad \theta \text{ an arbitrary real}\}$$

Each $E_k$ is an ellipse in tap space since it is expressible as a linear transformation of a circle. By $1_k$ we mean that 1 occurs in the $k$th position. The set $E \triangleq \cup_{-\infty}^{\infty} E_k$ are the points of global minima. These points are the ideal Nyquist responses (modulo a phase adjustment of the constellation).

A gradient search can only terminate on one of these circles of local minima. There are no spurious local minima. The only other stationary points are $c = \bar{0}$, which is a local maximum corresponding to the shut-down of the receiver and some points of unstable equilibrium "saddle points." We now substantiate these claims. The mathematical approach used in the remainder of this section is similar to that used in Sections VII and VIII. However, the demonstration here is much simpler.

### *5.1 Stationary points relative to overall system response*

To demonstrate the character of the stationary points, we first discuss the stationary behavior relative to $s$, from which the nature of the stationary points relative to $c$ will follow.

With respect to the conjugate coordinates $\bar{s}_k$, we take the partial derivative of $\phi$ and equate to zero to get

$$\left\{\frac{\partial\phi}{\partial\bar{s}_k} = 4\left(\sum_i |s_i|^2\right)s_k - \frac{6}{5}\frac{(L^2+1)}{(L^2-1)}|s_k|^2 s_k - 2\left(\frac{7L^2-13}{5(L^2-1)}\right)s_k = 0\right\}_{k=-\infty}^{\infty}.$$

So $s = \bar{0}$ is a solution. Dividing through by $s_k$ for $s_k \neq 0$ gives a very simple equation for the stationary points. In general, the stationary points are the vectors having the property that there are a finite number $M \geq 0$ of nonzero coordinates all $M$ of which are $(7L^2 - 13)[10M(L^2-1) - 3(L^2+1)]^{-1}$ in squared modulous. These stationary points are typed as

$M = 0$: $s = \bar{0}$, a local maximum
$M = 1$: global minima
$M \geq 2$: unstable equilibria.

The reasoning behind this typing of each case will now be given. Keep in mind the expression of $\phi(s)$ given in eq. (4).

The case $M = 0$.

This corresponds to $s = \bar{0}$, which is a local maximum. Simply note that sufficiently small perturbations of $\bar{0}$ serve to reduce the value of $\phi(s)$. The reason for this reduction is that, for a very small perturbation, the quartic effect is negligible relative to the quadratic one.

The case $M = 1$.

These points are loci of global minima. The global minimum cannot be attained if more than one component of $s$ is nonzero. Indeed, if $\hat{s}$ has more than one nonzero component then $\hat{s} \triangleq \bar{0}$, $(\sum |\hat{s}_i|^2)^{1/2}, \bar{0}$ gives $\phi(\tilde{s}) < \phi(\hat{s})$. Say that the $i$th component of $s$ is the only nonzero component. The function $\phi(s)$ is then minimized when $|s_i|^2 = 1$.

The case $M \geq 2$.

These points are unstable equilibria ("saddles"). The instability for a stationary point $s$ with $M \geq 2$ is shown by first decreasing $\phi(s)$ by a perturbation of two nonzero components of $s$ that leaves $\sum |s_i|^2$ invariant. Secondly, $\phi(s)$ is increased by a perturbation that simply increases the magnitude of a zero component by a sufficiently small positive number.

### *5.2 Stationary points relative to tap weights*

The results of Section 5.1 are only of incidental value since we are interested in the vector field relative to $c$ not relative to $s$. However, the results thus far can be interpreted to provide what we need, as we now explain.

The operation of convolution of $c$ with $h$ represents an invertible continuous function on tap space. Since $\phi(s)$ is a continuous real function of $s$, $\phi(s) = \phi(h * c)$ is also a continuous real function of $c$. Recall the very elementary fact that notions like local maximum, local minimum, and unstable equilibrium are defined as neighborhood properties in tap space. It is a property of continuity that the mappings $h*$ and $h^{-1}*$ leave invariant the entire system of neighborhoods. It is immediate from the results of Section 5.1 that the points in $E$ are the only points of stability in tap space when the taps evolve in accordance with the specified vector field.

For those uncomfortable with the above argument we give another level of detail. Say $\hat{s} = h * \hat{c}$ is a point of local minimum of $\phi$. This means that there is an open set in tap space containing $\hat{s}$, where $\phi(\hat{s})$ is the least number achieved. By convolution of elements of this open

set with $h$, one creates an open set about $\hat{c}$ on which $\phi(h * \hat{c})$ is the least number achieved. Local maxima and unstable equilibria are handled similarly.

## VI. A PRELIMINARY LOOK AT CONVERGENCE SPEED

### 6.1 *Interpretation of a published simulation*

To consider quantitatively the subject of convergence speed, we fix on a hypothetical example. Namely, we focus on a system with a transmission speed measured in tens of megabauds. Outage time accumulates when $P_e \geq 10^{-3}$, and is assumed to be limited to 150 seconds per year per hop (in a nominal system). The hypothetical channel is assumed to fade in accordance with the Rummler model.[11]

Let $P'(t)$ denote the probability of bit error that an *ideally* equalized system can provide at time $t$. Then $P'(t) \leq P(t)$, where $P(t)$ is the probability of bit error that is actually achieved at time $t$. For the purpose of discussion, assume that the clear air s/n is such that if $P(t)$ were identically equal to $P'(t)$, the outage objective would be roundly met. Suppose a fade is so severe that decision direction of the equalization process becomes impossible. When the fade subsides to the point where $P' \leq 10^{-3}$, the objective is to boot (or be booting) the equalizer so that $P \leq 10^{-3}$ occurs with a negligible time lag. An aggressive booting procedure, operating with an uncertain frequency-selective transfer characteristic, is viewed as a key element in achieving substantial outage reduction. The alternative of waiting for the dispersion to clear to the extent that a crude equalizer will open the eye is manifestly unacceptable.

The analysis of the booting process is difficult for two reasons. First, the extremal statistics of fade time dynamics are not well established. Second, even if such a model were available, it would be difficult to mathematically represent the time dynamics of an equalizer based on the Godard algorithm. However, if we assume that the time interval during which $P' > 10^{-3}$ lasts for a few seconds, then an equalizer booting time measured in tens of milliseconds would be negligible in terms of contributing to outage time. Indeed, even a 100-millisecond boot time would be negligible if the preponderance of the time occurs before the level $P' = 10^{-3}$ is down-crossed. Assuming that the channel transfer characteristic does not change appreciably during booting, we take a preliminary look at whether the quartic algorithm can boot an equalizer in tens of milliseconds.

Reference 2 reports simulations of transient responses from a cold start. The examples are for a voiceband application; however, they can be interpreted for a digital radio context. One of the examples is particularly interesting. (See Fig. 7d in Ref. 1.) Although 64 QAM is

not treated, rectangular constellations with 16 and 32 points are considered. The effect on the transient response of increasing from 16 to 32 is negligible. (This is expected because the constellation moments for $L^2 = 16$ points are already nearing their $L \to \infty$ asymptotes, as shown in the Appendix.) The channel used to generate the transient responses has as severe a dispersion as can be expected in the digital radio application. This statement is based on a rough indicator of dispersion, namely $\max_\omega |H(\omega)|^2/\min_\omega |H(\omega)|^2$. ($H(\omega)$ is the channel transfer characteristic.) The unimodal $|H(\omega)|^2$ had a higher indicator of dispersion than the most extreme of the 25,000 fades in a comprehensive library[7] generated from the Rummler model.[11]

The transient responses of Ref. 2 suggest that booting times of less than $10^5$ symbols may be possible. In the digital radio application at tens of megabauds, $10^5$ symbols are received in a few milliseconds.

A transient analysis of the algorithm is certainly an ambitious undertaking. However, it is possible to conduct a mathematical analysis of eq. (2) for a hypothetical, real, one-dimensional case. We sketch this analysis in the following subsection. By projecting the convergence behavior of interest into a simple, understandable context, useful insight is gained.

### 6.2 *Analysis of a related one-dimensional evolution*

In the much simpler domain of least-mean-square adaptation algorithms,[12] the transient behavior for the one-dimensional case is analyzed. Then a heuristic argument is made to extend the transient analysis to the higher-dimensional case. In the one-dimensional analysis of the Godard algorithm that follows, we will see how the corresponding MSE behavior of the algorithm compares with an MMSE evolution. The MMSE evolution assumes known data at the receiver.

In this one-dimensional case, both $h$ and $c$ are real scalars but the data is complex. In this subsection, a coordinate index is unnecessary so we write $c_i$ for $c_{[i]}$. The gradient algorithm is

$$c_{i+1} = c_i - \lambda \frac{\partial}{\partial c_i} (|z_i|^2 - |R|)^2. \tag{6}$$

For expositional simplicity in the sequel, we work with only the asymptotic form ($L \to \infty$) of the constellation moments. (Section V served to demonstrate that dealing with finite $L$ is not an essential complication. The Appendix shows the moment asymptotes are rapidly approached.) Compute for later use

$$\mu(c_i) \triangleq E(c_{i+1} - c_i \,|\, c_i) = -5.6\lambda h[(hc_i)^3 - hc_i] \tag{7a}$$

$$\sigma^2(c_i)^2 \triangleq E[(c_{i+1} - c_i)^2 \,|\, c_i]$$
$$= \lambda^2 h^2 [68.3(hc_i)^6 - 104(hc_i)^4 + 44.2(hc_i)^2]. \tag{7b}$$

Note that both $\mu$ and $\sigma$ are linear in $\lambda h$.

Were it not for the stochastic aspect, the evolution would be described by the nonlinear difference equation

$$c_{i+1} = c_i - 5.6\lambda h((hc_i)^3 - hc_i). \tag{8}$$

A crude representation of the evolution (8) with $\lambda$ small uses a deterministic differential equation. A more refined representation of (6) uses a stochastic differential equation. We look at both of these.

The deterministic differential equation is

$$\frac{dc}{dt} = -5.6\lambda h[(hc)^3 - (hc)], \tag{9a}$$

in the time scale where one unit equals one symbol time. The time, $T$, that it takes for $c$ to evolve from $c_o \neq 0$ to a target setting $c_f$ is easily seen to be

$$T = \frac{1}{11.2\lambda h^2} \ln\left(\frac{1 - (hc_o)^{-2}}{1 - (hc_f)^{-2}}\right). \tag{9b}$$

The corresponding formulae for the MMSE algorithm are

$$\frac{dc}{dt} = -2\lambda h(hc - 1) \tag{9c}$$

$$T = \frac{1}{2\lambda h^2} \ln\left(\frac{1 - hc_f}{1 - hc_o}\right). \tag{9d}$$

The formula (9d) is consistent with the statement in Ref. 12 that the time constant for the MMSE stochastic-gradient algorithm is $(2\lambda h^2)^{-1}$.

If one uses values in the right-hand side of (9b) and (9d) that are reflective of the digital radio application, the logarithmic term can be shown to be of little consequence in assessing order-of-magnitude effects. The latitude in being able to set $c_f$ so that $hc_f$ is only approximately 1 is crucial to taming the singularity. Reference 12 on MMSE explains that, in higher dimensions, $h^2$ is replaced by $(trace\ R/N)$, where $R$ is the channel autocorrelation matrix and $N$ is the number of equalizer taps. In data communication applications, a normalized form of the channel is often appropriate to account for AGC. In a one-dimensional context, AGC gives $hc = 1$, trivializing the equalization.

Refining (9a) to bring in the stochastic element of the evolution, we have

$$dc = \mu(c)dt + \sigma(c)d\beta(t), \tag{10}$$

where $(d\beta)/(dt)$ is a standard white-noise process. It is difficult to give a complete analysis of this equation; however, some results are possible.

A mathematical "experiment" was made to test the restoring action of the dynamic represented by (10). The mathematical tools in Ref. 13 were used. Set the tap $c$ at a very large value $c_o$ and consider the transit time to another large value $\gamma$. Assume $c_o \gg \gamma \gg c_f$. Under the deterministic evolution, (9a), the expected time until $\gamma$ is hit for the first time is proportional to $\gamma^{-2}$. With the stochastic dynamic, the expected hitting time is proportional to $\gamma^{-4}$.

As the tap setting $c$ nears the target region, the first-order term in the power series for $\mu(c)$ and $\sigma^2(c)$ is linear and constant, respectively. This limiting evolution is that of the elastically bound particle (also called Orstein-Uhlenbeck[14]). A complete transient analysis of the dynamics of the elastically bound particle is classical.[14] We have

$$E[hc(t) - 1 \mid c(0) = c_o] = (hc_o - 1)e^{-11.2\lambda h^2 t} \tag{11a}$$

$$\mathrm{Var}[hc(t) - 1 \mid c(0) = c_o] = 0.381\lambda h^2(1 - e^{-22.4\lambda h^2 t}). \tag{11b}$$

We are assuming the quartic algorithm is only for bootstrapping, so $0.381\lambda h^2$ does not correspond to the equilibrium variance.

It is interesting to contrast with MMSE, for which the expected time from start to target is available in closed form using the method of Ref. 13. We get

$$T = \frac{1}{\lambda h^2 + 1.4\lambda^2 h^4}\left[\frac{1 - \left(\frac{1 - hc_f}{1 - hc_o}\right)^{1+\frac{5}{7\lambda h^2}}}{1 + \frac{5}{7\lambda h^2}} + \frac{1}{2}\ln\left(\frac{1 - hc_f}{1 - hc_o}\right)\right]$$

$$\sim \frac{1}{2\lambda h^2}\ln\left(\frac{1 - hc_f}{1 - hc_o}\right) \ (\lambda \text{ small}).$$

Also,

$$E(hc(t) - 1 \mid c(0) = c_o) = (hc_o - 1)e^{-2\lambda h^2 t} \quad \text{for each } t, \tag{11c}$$

and

$$\mathrm{Var}(hc(t) - 1 \mid c(0) = c_o) \sim (hc_o - 1)^2 e^{-1.2\lambda h^2 t} \quad \text{as } t \to \infty. \tag{11d}$$

Noise and quantization effects, which are not included, will predominate for large $t$ and thus serve to bound the MMSE variance above zero.

Interestingly, for both the MMSE and quartic algorithm, the exponential decay that is observed in the simple deterministic analysis is maintained when stochastic effects are included. Evolution under the quartic potential compares favorably with that of the quadratic. However, the apparent advantage of the quartic of a factor of 5.6 in time constant is illusory, as we next discuss.

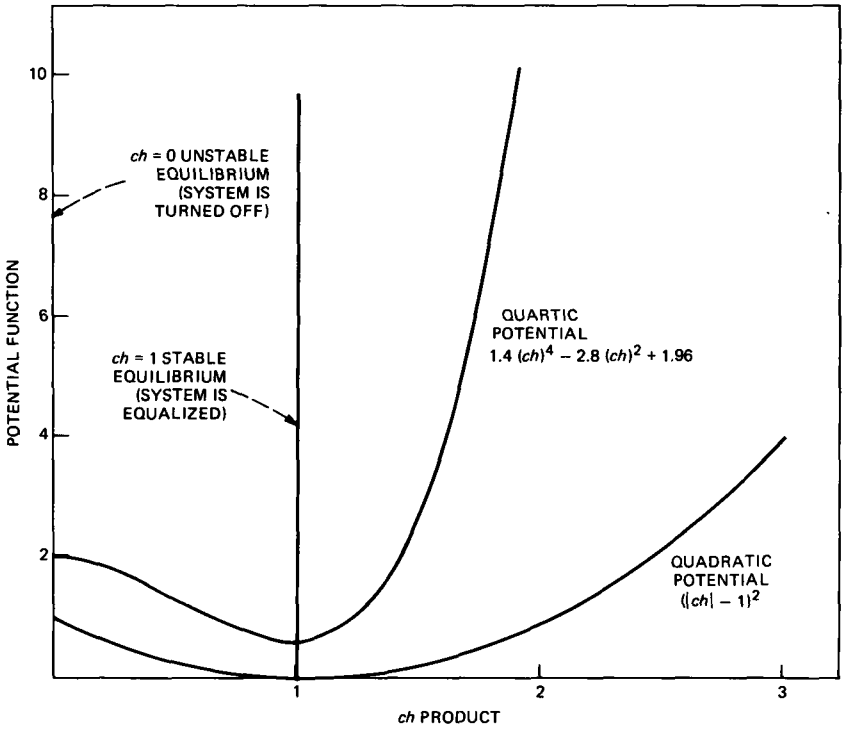


Fig. 2—Potential functions for simple one-dimensional case.

Relation (8a) suggests that one should make $\lambda$ large to reduce the transit time. However, $\lambda$ must be set carefully. The differential equation loses its effectiveness as an approximation to (8) once $\lambda$ gets too large. An analysis of (8) points out that, for $\lambda$ sufficiently large,

$$|c_{i+1}| > |c_i|,$$

which is a disastrous instability. The wall of the potential well for Godard's algorithm is quartic while, for MMSE, it is quadratic. (See Fig. 2 to contrast the quartic and quadratic potentials.) Consequently, the quartic algorithm requires a smaller $\lambda$ to avoid instability than MMSE requires. Indeed, in the simulations of Ref. 2 it was noticed that a smaller value of $\lambda$ was needed. As $c_i$ approaches the target region, one would like $\lambda$ small to encourage stepping *into* rather than over the target region. A key area of future study is to determine a *dynamic* procedure for prudent setting of $\lambda$.

### *6.3 A heuristic discussion of transient behavior*

The results of the previous subsection require refinement to obtain a more global description of the behavior of the trajectories of (6).

More importantly, the vector algorithm needs to be analyzed and that appears to be formidable. These are items for future research. At present we are limited to drawing on what we have developed in Sections V and 6.2.1 to express our current intuition of the qualitative nature of tap evolution: *Far from the target region, there are saddle points representing loci where more than one target region is equally accessible. The evolution is not stymied as the strong random effect forces a choice. Still far from the target region, there is a very strong trend toward the target. The motion slows as the target is approached and becomes that of a particle elastically bound to the elliptical bull's-eye corresponding to the Nyquist responses. Close to the target, the radial motion is not essentially different from an Orstein-Uhlenbeck evolution, except in one respect. The evolution has a tangential indifference that is of no consequence since phase coherence is left for an auxiliary process. The $\overline{0}$ tap setting is an unstable equilibrium that is to be avoided (and that is not difficult). To the extent that the vector tap does not begin too close to zero, the transit time to target would seem to be dominated by the Orstein-Uhlenbeck-like motion.*

## VII. REMOVING PHASE AMBIGUITY

A useful feature of the quartic algorithm that we have been discussing is that equalizer convergence does not need carrier recovery. As explained in Ref. 2, the tracking of carrier phase can be carried out using a decision-directed phase-locked loop that will converge once equalization has taken place. For digital radio applications, this feature implies a significant immunity of the equalization process to frequency offset and phase jitter.

On the other hand, if a digital radio system were designed with highly stable oscillators, could we employ a quartic algorithm providing for coherent recovery without a phase-locked loop? After all, standard, decision-directed MMSE equalization provides, upon convergence, for coherent recovery of the signal constellation. This result holds, in principle, under the idealized assumption that the channel is linear and time invariant. In practice, depending on the degree of phase jitter and frequency offset, a phase-locked loop may or may not be required. In this section, we seek to provide an analogous result for nondecision-directed equalization. Specifically, we demonstrate the existence of a potential function that provides for phase recovery as part of equalization. Of course, a QAM constellation is left invariant by 90 degree rotations, so the more precise meaning of the term "phase recovery" is phase recovery modulo 90 degrees.

For expositional simplicity, we develop the potential function for the asymptote of a QAM constellation with infinitely many points. The approach to defining corresponding potentials for finite constel-

lations is the same as for the asymptotic case. The limiting form, as $L \to \infty$, of the potential function given in equation (5) is

$$\phi(s) = 2\left(\sum_i |s_i|^2\right)^2 - 0.6 \sum_i |s_i|^4 - 2.8 \sum |s_i|^2 + 1.96.$$

We will show how to modify $\phi(s)$, but first, for a backdrop, we discuss a much simpler situation in which phase recovery is obtained.

### 7.1 *Orienting a rotated but otherwise perfect constellation*

We have seen that the stochastic gradients with respect to $c$ of $E|z_n|^4$ and $E|z_n|^2$ are readily accessible. From (1) and the ensuing discussion, we have that for appropriate choice of A and B, tap settings evolving in accordance with the gradient field of $AE|z_n|^4 + BE|z_n|^2$ converge to an optimal equalizer up to a rotation. Obviously, Re $Ez_n^4$ also has a readily accessible stochastic gradient. Moreover, Re $Ez_n^4$ may be useful for phase recovery, as we next indicate.

It is easy to see that $Ea_n^4$ is a negative number. Let $a_n' = e^{j\theta}a_n$, where $\theta$ is an arbitrary phase displacement that does not depend on $n$. It follows that

$$\eta(\psi) = E\ \mathrm{Re}(e^{j\psi}a_n')^4$$

is minimized when $\psi = -\theta(\mathrm{mod}\ \pi/2)$. These are the only minima, whereas $\psi + \theta = \pi/4\ (\mathrm{mod}\ \pi/2)$ are the only maxima. Consequently, a tap rotating according to the gradient field of $\eta(\psi)$ comes to a stable state when the constellation is correctly oriented.

Based on what we have discussed thus far, one might suspect the existence of a potential of the form $E(A'|z_n|^4 + B'|z_n|^2 + C'$ Re $z_n^4)$ whose only points of stability are ideal Nyquist responses with recovered carrier. Such potentials exist, as we now show.

### 7.2 *Equalization with orientation*

In what follows, positive parameters $\nu$ and $\mu$ are introduced in the potential function, $\phi(s)$, as follows:

$$\phi(s) = 2\ (\sum |s_k|^2)^2 - 2.8 \sum |s_k|^2 - \mu \sum |s_k|^4 - 2\nu\ \mathrm{Re} \sum s_k^4.$$

Later we will see that $\nu$ and $\mu$ can be set to get the tap evolution desired. Namely, we can obtain an evolution whose only points of stability are of the form $\bar{0}\epsilon\bar{0}$, $(\epsilon^4 = 1)$.

The gradient of $\phi(s)$ with respect to the conjugate coordinates is

$$\nabla\phi_{\bar{s}_i} = 4 \sum |s_k|^2 s_i - 2.8 s_i - 2\mu |s_i|^2 s_i - 4\nu \bar{s}_i^3. \tag{12}$$

The solutions are the stationary points. The Hessian matrix is denoted $\mathcal{H} = (H_{ij})$ (where $H_{ij} = (\partial^2\phi)/(\partial\bar{s}_i\partial s_j)$). We have

$$H_{ij} = 4 \sum_k |s_k|^2 + 4|s_i|^2 - 2.8 - 4\mu|s_i|^2 \quad \text{for} \quad i = j$$
$$= 4\bar{s}_j s_i \quad \text{for} \quad i \neq j. \tag{13}$$

As in Section 5.2, $\bar{0}$ is easily seen to be a local maximum. Expressing $s_i$ as $|s_i| e^{j\theta_i}$, eq. (12) for the non-null stationary points becomes

$$-4\nu|s_i|^2 e^{-4j\theta_i} - 2\mu|s_i|^2 - 2.8 + 4\sum|s_k|^2 = 0$$

$$\text{or} \quad |s_i|^2 = \frac{4\sum_k |s_k|^2 - 2.8}{4\nu e^{-4j\theta_i} + 2\mu}. \tag{14}$$

From the nonnegativity of $|s_i|^2$, we conclude that

$$e^{-4j\theta_i} = \pm 1.$$

But $e^{-4j\theta_i} = -1$ cannot be associated with a local minimum. Just look at (14) and notice $e^{-4j\theta_i} = e^{+4j\theta_i} = -1$ implies $\text{Re}\sum_k s_k^4 > 0$ so the mapping $s \to \cdots s_{i-1}, s_i e^{j\zeta}, s_{i+1} \cdots$ reduces the value of $\phi$. The local minima of $\phi$ must have $e^{j4\theta_i} = +1$. These minima satisfy

$$|s_i|^2 = \frac{4\sum|s_\mu|^2 - 2.8}{4\nu + 2\mu}. \tag{14a}$$

Each minimum has all nonzero coordinates of equal modulus, all equal to the right-hand side of (14). Say there are $M$ nonzero coordinates; then

$$|s_i|^2 = \frac{1.4}{2M - 2\nu - \mu}.$$

To ascertain whether the stationary points are local minima, or points of instability (saddle points), we need to determine the nature of the Hessian at the stationary points. To effectively deal with the Hessian, it is mathematically convenient to permute coordinates so that the coordinates 1 through $M$ are the ones for which (14a) holds. Some notation is also needed. $0_{p,q}$ represents a matrix with $p$ rows and $q$ columns in which each element is zero. $I_p$ denotes a $p \times p$ identity matrix. The Hessian is

$$\mathscr{H} = \frac{2.8}{2M - \mu - 2\nu}\left\{\begin{bmatrix} 0_{\infty,\infty} & 0_{\infty,M} & 0_{\infty,\infty} \\ 0_{M,\infty} & (2\nu - \mu)I_M & 0_{M,\infty} \\ 0_{\infty,\infty} & 0_{\infty,M} & 2(\nu + \mu)I_\infty \end{bmatrix} + 2s\bar{s}'\right\}. \tag{15}$$

Notice $\mathscr{H}$ is expressed as the sum of a diagonal matrix and a dyad. The nonzero elements of $s$ in eq. (15) are all $\pm 1$ or $\pm j$. The special structure of $\mathscr{H}$ allows the spectrum of $\mathscr{H}$ to be easily found. The nonzero eigenvalues are

$$\frac{0.7(2 + 2\nu - \mu)}{2M - 2\mu - 2} \text{ of multiplicity one}$$

$$\frac{0.7(2\nu - \mu)}{2M - 2\mu - 2} \text{ of multiplicity } M - 1$$

$$\frac{0.7(\mu + 2\nu)}{2M - 2\mu - 2\nu} \text{ of infinite multiplicity.}$$

It remains now to choose $\mu$ and $\nu$ so that the only stable equilibria are of the form $\bar{0}\epsilon\bar{0}$, where $\epsilon^4 = 1$.

For $|s_i| = 1$ when $M = 1$ choose $\mu + 2\nu = 0.6$. From the spectrum of eigenvalues it follows that if we have

$$2 - \mu + 2\nu > 0 - \mu + 2\nu < 0,$$

then $M = 1$ gives a positive semidefinite Hessian and $M > 1$ gives an indefinite Hessian. For example, $\mu = 0.45$ and $\nu = 0.075$ satisfies all requirements. So the only stable equilibria of $\phi(s)$ with $\mu = 0.45$ and $\nu = 0.075$ are of the form $\bar{0}\epsilon\bar{0}$ with $\epsilon^4 = 1$.

Again, as in Section 5.2.1, we have described the stationary behavior of the gradient field with respect to $s$ and not with respect to $c$. The argument extends to tap space in the same manner as in Section 5.2.2.

## VIII. ALGORITHM FOR CROSS-POLARIZATION CANCELLATION AS WELL AS EQUALIZATION

In this section we develop the theory for a cross-polarization cancellation algorithm. We will establish that a $2 \times 2$ matrix equalizer will converge so that both receiver outputs are free of Intersymbol Interference (ISI) and cross-polarization interference. There is a possibility that, despite the perfect decoupling, one or both polarizations may be transposed. The taps evolve in accordance with the gradient of a vector potential that will be introduced shortly. Upon convergence, phase needs to be recovered by a pair of phase-locked loops. This transposition ambiguity is easily resolved in practice. For example, the polarizations may be "tagged" by the scrambling process. When necessary, the procedure can be reinitialized to attempt to avoid locking onto the undesired polarization.

Some notation needs to be introduced. We need a two-dimensional setting to account for horizontally and vertically polarized signals. Here $c$ and $h$ are $2 \times 2$ matrices. The vectors $(z_H, z_V)$ and $(a, b)$ are related as follows:

$$\begin{pmatrix} z_H \\ z_V \end{pmatrix} = \begin{pmatrix} c_{11} & c_{12} \\ c_{21} & c_{22} \end{pmatrix} * \begin{pmatrix} h_{11} & h_{12} \\ h_{21} & h_{22} \end{pmatrix} * \begin{pmatrix} a \\ b \end{pmatrix}.$$

The individual elements of $z_H$, $z_V$, $a$ and $b$ are denoted by subscripts. We use $s$ to denote the matrix

$$c * h = \begin{pmatrix} c_{11} * h_{11} + c_{12} * h_{21} & c_{11} * h_{12} + c_{12} * h_{22} \\ c_{21} * h_{11} + c_{22} * h_{21} & c_{22} * h_{21} + c_{22} * h_{22} \end{pmatrix}.$$

The matrix $h$ is assumed to be nonsingular so that $h^{-1}$ exists

$$\left( h^{-1} * h = \begin{pmatrix} \overline{0}, 1_0, \overline{0} & \\ \overline{0} & \overline{0}, 1_0, \overline{0} \end{pmatrix} \right).$$

The components of the vector $(a, b)$ represent the QAM data sequence driving the horizontal and vertical polarizations. Of course, the elements of $a$ and $b$ are all independent.

We employ a vector criterion; specifically we want

$$\begin{pmatrix} \min\limits_{(c_{11}, c_{12})} E(|z_{Hn}|^2 - E|a_n|^4)^2 \\ \min\limits_{(c_{21}, c_{22})} E(|z_{Vn}|^2 - E|b_n|^4)^2 \end{pmatrix}.$$

The advisability of this vector criterion will become apparent. Notice optimization of these two components proceed independently of each other in that the first component involves $c_{11}$ and $c_{12}$ while the second involves $c_{21}$ and $c_{22}$.

We next show how to express these two expectations in terms of the components of $s$ (denoted $s_{ij}(k) i, j = 1, 2$) and the moments of $a_n$ and $b_n$. By symmetry it will be enough to make this demonstration for the first expectation. Again we normalize $E|a_n|^2 = E|b_n|^2 = 1$. Since

$$z_{Hn} = \sum_k (s_{11}(k) a_{n-k} + s_{12}(k) b_{n-k}),$$

we obtain

$$E|z_{Hn}|^4 = E \left\{ \sum_k \sum_l \sum_p \sum_q (s_{11}(k) a_{n-k} + s_{12}(k) b_{n-k})(\bar{s}_{11}(l) \bar{a}_{n-l} + \bar{s}_{12}(l) \bar{b}_{n-l}) \times (s_{11}(p) a_{n-p} + s_{12}(p) b_{n-p})(\bar{s}_{11}(q) \bar{a}_{n-q} + \bar{s}_{12}(q) \bar{b}_{n-q}) \right\}.$$

Consider the product inside the quadruple sum. Of the 16 terms only the six involving $a_{n-k}\bar{a}_{n-l}a_{n-p}\bar{a}_{n-q}$, $a_{n-k}\bar{a}_{n-l}b_{n-p}\bar{b}_{n-q}$, $a_{n-k}\bar{b}_{n-l}b_{n-p}\bar{a}_{n-q}$, $b_{n-k}\bar{b}_{n-l}b_{n-p}\bar{b}_{n-q}$, $b_{n-k}\bar{b}_{n-l}a_{n-p}\bar{a}_{n-q}$ and $b_{n-k}\bar{a}_{n-k}a_{n-p}\bar{b}_{n-q}$ give nonzero expectations. This simplification follows by recalling that $a$ and $b$ are independent and $Ea^j = Eb^j = \overline{0}$ for $j = 1, 2, 3$. Concerning the six terms, we note that the last three terms become the same as the first three if we transpose $a$ and $b$. Moreover, the second and third terms are exactly the same since the only apparent differences are in the labelings of indices that are being summed. So we need to ascertain

only the first two of the six expectations and symmetry will give the rest. The two sums are already available. Namely,

$$\sum_k \sum_l \sum_p \sum_q E(s_{11}(k)a_{n-k}\bar{s}_{11}(l)\bar{a}_{n-1}s_{11}(p)a_{n-p}\bar{s}_{11}(q)\bar{a}_{n-q})$$
$$= (E|a_n|^4 - 2)\sum_k |s_{11}(k)|^4 + 2\left(\sum |s_{11}(k)|^2\right)^2 \quad (16)$$

and

$$\sum_k \sum_l \sum_p \sum_q E(s_{11}(k)a_{n-k}\bar{s}_{11}(l)\bar{a}_{n-l}s_{12}(p)b_{n-p}\bar{s}_{12}(q)\bar{b}_{n-q})$$
$$= \left(\sum_k |s_{11}(k)|^2\right)\left(\sum_k |s_{12}(k)|^2\right). \quad (17)$$

Using the aforementioned symmetry gives, for the six terms comprising $E|z_{Hn}|^4$, four copies of (17), and in addition to (16), its counterpart with $s_{11}$ and $s_{12}$ interchanged. To compute $E(|z_{Hn}|^2 - E|a_n|^4)^2$, we also need $E|z_{Hn}|^2 = E|a_n|^2(\sum|s_{11}(k)|^2 + \sum|s_{12}(k)|^2)$. At this point we can substitute all the terms making up $E(|z_{Hn}|^2 - E|a_n|^4)^2$ and rearrange to get

$$E(|z_{Hn}|^2 - E|a_n|^4)^2 = 2(\sum|s_{11}(k)|^2 + \sum|s_{12}(k)|^2)^2$$
$$+ (E|a_n|^4 - 2)(\sum|s_{11}(k)|^4 + |s_{12}(k)|^4)$$
$$-2E|a_n|^4(\sum|s_{11}(k)|^2 + \sum|s_{12}(k)|^2) + (E|a_n|^4)^2. \quad (18)$$

We introduce a new sequence $S(k)$ obtained by alternating $s_{11}(k)$ and $s_{12}(k)$ elements. Thus $S(0) = s_{11}(0)$, $S(1) = s_{12}(0)$, $S(2) = s_{11}(1)$, $S(3) = s_{12}(1)$, $\cdots$ and $S(-1) = s_{12}(-1)$, $S(-2) = s_{11}(-1)$, $S(-2) = s_{12}(-2)$, $S(-3) = s_{11}(-2)\cdots$. Then (18) becomes the same as (5) with $S$ replacing $s$. The invertibility of $h$ enables us to achieve the optimum value.

The stationary behavior of (18) now follows immediately from the results in Section 5.1. The minimizing $c_{11}$ and $c_{12}$ satisfy

$$\begin{pmatrix} c_{11} * h_{11} + c_{12} * h_{21} \\ c_{11} * h_{12} + c_{12} * h_{22} \end{pmatrix} = \begin{pmatrix} \bar{0} \\ \bar{0}e^{j\theta}\bar{0} \end{pmatrix} \quad \text{or} \quad \begin{pmatrix} \bar{0}e^{j\theta}\bar{0} \\ \bar{0} \end{pmatrix}.$$

We are now in a predicament analogous to that at the end of Section 5.1. As the results stand, they apply to $s$, not to $c$. A very straightforward vector matrix extension of the argument in Section 5.1 gives the results desired for $c$.

## IX. FINITE NUMBER OF TAPS

Thus far, the theory has been idealized in the sense that infinitely many taps were assumed. Can we be sure that, by using a large number of taps, an equalizer will behave in essentially the same way as an

infinite tap equalizer? Unlike MMSE theory, the theory of the quartic algorithm with finitely many taps is awkward to treat analytically. Partial, positive results are available and are conveyed here.

The next subsection enhances the quartic algorithm to alleviate one of the difficulties arising with a finite equalizer. The following subsection mentions very special related examples, where, with a finite number of taps, the convergence theory is complete and satisfactory. The next subsection reviews the status of the finite tap issue.

The related topic of quantifying the *number* of taps needed in digital radio applications seems best addressed by computer-aided analysis (as with MMSE equalization[15]). We emphasize that, in the digital radio application, we are *not* aiming to equalize pathological $H(\omega)$ with severe in-band nulls (and consequently an unreasonable number of taps to approximate $h^{-1}$). Rather, as indicated in Section VI, the interest is in equalizing when $H(\omega)$ can support a $P_e'$ of the order of $10^{-2}$. For implementations, one would expect to use fractionally spaced rather than synchronously spaced taps. A numerical example is reported in Section 9.4.

### 9.1 *Centering the tap weight distribution*

The feature that the algorithm has no preference as to which tap should be the reference tap implies that, with finitely many taps, the tap weight distribution could crowd to one end of the equalizer. To avoid a lopsided tap-weight distribution one could periodically (say every few hundred symbols) have computed the center of gravity of the tap weights and then shift the weights to situate the balance point as close as possible to the center tap. When the quartic algorithm is in use, outage time is registering, so no additional outage is caused by shifting. The centering helps approximate the effect of infinitely many taps that the theory has required. A computationally simpler alternative to the center of gravity method is to periodically compare the weights of the first and last tap, and then shift tap weights by one in the direction of the least weight.

### 9.2 *Special-case convergence*

Equalization when accurate estimates of the data are not available has been discussed for a very different algorithm in Ref. 5. That paper analyzes the case where the channel is perfect but the equalizer is misaligned. It is shown that, for certain tap initializations, convergence to an undesirable setting is possible. For the Godard algorithm, there is no problem when the channel is perfect and the equalizer is misaligned (arbitrarily). To show that there is no difficulty, we can make use of the analysis in Section V. In this case, $s_j = c_j$. The finiteness of

the number of taps does not alter the argument. Convergence to the optimum tap setting is guaranteed.

For the second example, in the potential function of (4), interpret $s$ (and $h$ and $c$) as a discrete Fourier transform. Then it is not difficult to show that, within this modular context, convergence of $c$ occurs. This is an artificial construct. However, a variation of this example of a finite tap equalizer may have some utility. Prospective application is not within the scope of equalization procedures of the kind that leave the transmitted signal inviolate. Rather, the application is associated with the equalizer booting methods of the kind that use intervals of periodic training sequences. (The DFT is the key to modeling such equalizers.[16]) The motivation for using quartic criteria such as in eq. (3) is that an immunity to frequency offset is anticipated. This type of equalization, which uses both a quartic potential and training sequence, has arisen in concurrent research by A. A. M. Saleh and the author.

### *9.3 Status*

The issue of the effect of limiting the number of taps is, at bottom, the question of whether with sufficiently many taps and with centering as in Section 9.1 the evolution of the quartic error departs negligibly from the infinite tap case. Godard[1] does not discuss the issue of limiting the number of taps.

For a given application, one could circumscribe a universal ensemble of desired $h^{-1}$ and then choose the number of taps large enough so the approximation error is uniformly negligible, i.e., so that the omitted taps are essentially zero anyway. At each point in time, the taps that can evolve do so in such a way that the infinitesimal tap evolution is the same as the unlimited tap case. The taps that are omitted are essentially preset at their optimum values ($\approx zero$). The random component of the evolution serves to mask the effect of any perturbations of the infinite tap vector field that is caused by limiting the number of taps.

The material presented so far supports that, with a sufficiently large number of taps (and employing a weight centering procedure), the convergence properties of the Godard algorithm differ negligibly from what is predicted for the infinite tap equalizer. However cogent the supporting evidence, a mathematically rigorous argument has not been given. The understanding of the finite tap issue is refined by a numerical example that concludes this section.

### *9.4 ISI versus number of taps*

With the aid of the computer one can take a deeper look at finite tap behavior. A computer program has been written to solve the *deterministic* equation of tap evolution

$$c_{[n+1]} = c_{[n]} - \lambda \nabla \phi(c_{[n]}).$$

One can track the MSE from start, $MSE_{[o]}$, to equilibrium, $MSE_{[\infty]}$. The potential function, $\phi$, could be MMSE (with known data) or the quartic (with unknown data). The number of levels and the timing epoch are potential function parameters. For numerical work, some of the idealizing assumptions were dropped and we generalized to incorporate important practical effects. Namely, the equalizer can have fractionally spaced taps and the transmitted pulse can be raised cosine with arbitrary roll-off factor.

It is beyond the scope of this paper to include a comprehensive numerical study. We do, however, report the result of one interesting computer experiment. Figure 3(a) expresses $MSE_{[\infty]}$ versus the number of taps for some anecdotal cases of multipath fade. The fade characteristics are in accordance with the Rummler model[11] for multipath with midband notches in the range 16 to 22 dB. The Rummler phase parameter is zero and the scale parameter is inconsequential, as the affect of additive noise is neglected. See Fig. 3b. The roll-off is 25 percent, and the fractional spacing is half that of synchronous equalization. The timing epoch is optimized. The curves were generated for $L = \infty$ (as we are primarily interested in large constellations and the characteristics are insensitive to changes in $L$ for $L$ large). Computations were made for 3, 5, 7, and 9 taps. The curves shown are solid merely for interpolating to the even ordinates; of course there is no meaning to a noninteger number of taps.

The original intent in generating the characteristics in Fig. 3 was to compare $MSE_{[\infty]}$ for the quartic and quadratic potentials. However, once the points were determined it was discovered that there was no difference observable to the eye! In this computer experiment the quartic equilibrium is essentially as good as the quadratic one in minimizing MSE. This virtual equality is stronger than what is required of the quartic algorithm. We only desire that the quartic equilibrium be close enough to the quadratic equilibrium so as to create the option of switching to MMSE evolution once good decisions are available.

## X. DISCUSSION

We have delved into the theoretical aspects of quartic algorithm. The results obtained included stability with respect to tap initialization (Section V), equalization including acquisition of phase in systems employing highly stable oscillators (Section VII), and cancellation of crosspolarization interference (Section VIII). Section VI discussed convergence times which are of interest in bootstrapping digital radio systems. Section IX suggests that with centering, and with enough

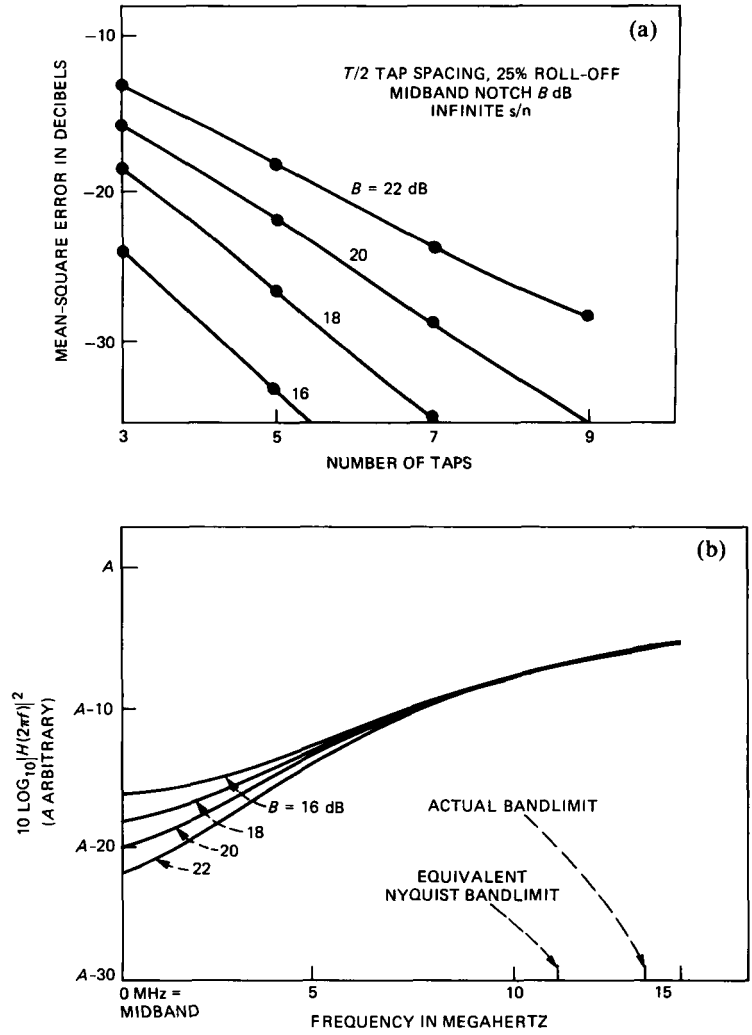


Fig. 3—(a) Steady-state mean-square error versus number of taps for quartic criterion. (b) Power transfer characteristics of channels used in computation of mean-square error$_{[\infty]}$ for quartic algorithm.

taps, the finite tap equalizer may perform essentially as well as the infinite tap equalizer.

It is premature to answer the question of whether digital radio systems should be designed to provide for self-alignment without inserting media probing signals in the transmitted signal. However, the results that have been elucidated thus far are promising enough to warrant further study.

The electronics needed for implementation needs to be assessed.

Ideally, one would like to update taps every symbol interval. Then convergence speed is high and the operation of the algorithm is less vulnerable to the assumption that the channel is unchanged during booting. It is conceivable to implement such an algorithm with special-purpose hardware. However, this now may prove unrealistic from an economic standpoint. (In time the economic issue will disappear.) One could slow the algorithm, updating every 10 or 100 symbols, to obtain a more realistic implementation. By slowing the algorithm, convergence speed, rather than economics, becomes the issue. The question of how fast an algorithm is needed is particularly difficult to address, especially for cross-polarization cancellation, because of the lack of data on coupling dynamics. One could strive to compensate for slowness by developing good, adaptive, step-size algorithms. These are all items for future study.

The best approach for future investigations of the usefulness of quartic algorithms in digital radio would seem to require inclusion of simulation and/or experimentation aimed at specific applications. Ultimately, it is necessary to include additive noise in such evaluations.

## XI. ACKNOWLEDGMENTS

The author gratefully acknowledges helpful interactions with N. Amitay, R. D. Gitlin, L. J. Greenstein, M. I. Reiman, A. A. M. Saleh, J. Salz, A. Weiss, J. J. Werner, and Y. S. Yeh.

## REFERENCES

1. D. Godard, "Self-Recovering Equalization and Carrier Tracking in Two-Dimensional Data Communication Systems," IEEE Trans. Commun., *COM-28* (November 1980), pp. 1867–75.
2. D. Godard, "A 9600 Bit/s Modem for Multipoint Communications Systems," IEEE NTC 1981 Conf. Rec., New Orleans, LA., November 29–December 3, pp. B3.3.1–B3.3.5.
3. Y. Sato, "A Method of Self-Recovering Equalization for Multilevel Amplitude-Modulation Systems," IEEE Trans. Commun., *COM-23* (June 1975), pp. 679–82.
4. J. E. Mazo, "Analysis of Decision-Directed Equalizer Convergence," B.S.T.J., *59*, No 10 (December 1980), pp. 1857–76.
5. A. Beneniste and M. Goursat, "A Gain and Phase Identification Procedure: Blind Adjustment of a Recursive Equalizer," IEEE Inform. Theory Symp., Grignano, Italy, June 1980.
6. A. Benveniste and M. Goursat, "Blind Equalizers," INRIA, Rapports de Richerche, No. 219, July 1983.
7. G. J. Foschini and J. Salz, "Digital Communications Over Fading Radio Channels," B.S.T.J., *62*, No. 2, Part 1 (February 1983), pp. 429–56.
8. J. Salz, "Optimum Mean-Square Decision Feedback Equalization," B.S.T.J., *52*, No. 8 (October 1973), pp. 1341–73.
9. D. D. Falconer and G. J. Foschini, "Theory of Minimum Mean-Square-Error QAM Systems Employing Decision Feedback Equalization," B.S.T.J., *52*, No. 10 (December 1973), pp. 1821–48.
10. A. C. Salazar, "Design of Transmitter and Receiver Filters for Decision Feedback Equalization," B.S.T.J., *53*, No. 3 (March 1974), pp. 503–23.
11. W. D. Rummler, "A New Selective Fading Model: Application to Propagation Data," B.S.T.J., *58*, No. 5 (May–June 1979), pp. 1032–71.
12. B. Widrow and J. M. McCool, "A Comparison of Adaptive Algorithms Based on the

Methods of Steepest Descent and Random Search," IEEE Trans. Antennas and Propagation, *AP-24*, No. 5 (September 1976), pp. 615–37.
13. S. Karlin and H. M. Taylor, *A Second Course in Stochastic Process*, New York: Academic Press, 1981, Chapter 15.
14. L. Arnold, *Stochastic Differential Equations*, New York: Wiley-Interscience, 1974.
15. N. Amitay and L. J. Greenstein, "Multipath Outage Performance of Digital Radio Receivers Using Finite-Tap Adaptive Equalizers," IEEE Trans. Commun., *COM-32* (May 1984), pp. 597–608.
16. K. H. Mueller and D. A. Spaulding, "Cyclic Equalization—A New Rapidly Converging Equalization Technique for Synchronous Data Communication," B.S.T.J., *54*, No. 2 (February 1975), pp. 370–406.

## APPENDIX

### *Even-Order Moments of QAM Constellations*

The moments $E|a_i|^4$ for constellations with $L^2$ points are required in the paper. A general procedure for calculating $E|a_i|^N$ ($N$ even) is as follows: Write a recursion in $L$ for $m_N(L) \triangleq E(\mathrm{Re}\ a_i)^N$. The recursion can be solved using transforms. Straightforward algebra can be used to obtain $E|a_i|^N$ from $m_N(L)$, e.g.,

$$E|a_i|^2 = 2m_2$$

$$E|a_i|^4 = (m_4 + m_2^2)$$

$$E|a_i|^6 = (m_6 + 3m_4m_2)$$

$$E|a_i|^8 = 2(m_8 + 4m_6\bar{m}_2 + 3m_4^2).$$

Normalizing $E|a_i|^2 = 1$ and following the above suggestion for $N = 4$ gives

$$E|a_i|^4 = \frac{7L^2 - 13}{5(L^2 - 1)}.$$

For a constellation with a large number of points it is useful to have the asymptotic ($L \to \infty$) form for the moments. The result is

$$\lim_{L\to\infty} m_N(L) = \frac{1}{2A}\int_{-A}^{A} |\zeta|^N d\zeta = \frac{A^N}{N+1}.$$

Since $E|a_i|^2 = 1$ we have $A = \sqrt{3/2}$. Therefore

$$E|a_i|^4 \to 7/5$$

$$E|a_i|^6 \to 81/35$$

and $$E|a_i|^8 \to 747/175.$$

These asymptotes were used in composing (7b). As a check compare $E|a_i|^4$ in the exact and asymptotic form. Note $E|a_i|^4$ asymptotes quickly. For $L^2 = 16$ points $E|a_i|^4 = 1.32$ as compared to 1.4 for an infinite point constellation.

## AUTHOR

**Gerard J. Foschini,** B.S.E.E., 1961, Newark College of Engineering, Newark, NJ; M.E.E., 1963, New York University, New York; Ph.D. (Mathematics), 1967, Stevens Institute of Technology, Hoboken, NJ; AT&T Bell Laboratories, 1961—. Mr. Foschini initially worked on real-time program design. For many years he worked in the area of communication theory. In the spring of 1979 he taught at Princeton University. Mr. Foschini has supervised planning the architecture of data communications networks. Currently, he is involved with optical communication research. Member, Sigma Xi, Mathematical Association of America, IEEE, New York Academy of Sciences.